

Enhanced Low Temperature Performance of LiFePO₄ Cathode with Electrolyte Modification

Borong Wu¹, Yonghuan Ren¹, Daobin Mu^{1,*}, Cunzhong Zhang¹, Xiaojiang Liu², Feng Wu¹

¹ Beijing key laboratory of Environment Science and Engineering, School of Chemical Engineering and Environment, Beijing Institute of Technology, Beijing 100081, China.

² Institute of Electric Engineering, China Academy of Engineering Physics, Mianyang 621900, China.

*E-mail: mudb@bit.edu.cn

Received: 20 April 2013 / Accepted: 11 May 2013 / Published: 1 June 2013

Electrolyte conductivity and solid electrolyte interphase (SEI) film are two key factors that affect the low temperature performance of LiFePO₄ battery. In this work, the enhancement of conductivity is realized through optimizing the proportion of solvents by mass triangle model. SEI modification is achieved by adding film-forming agent of Li₂CO₃ in the high conductivity electrolyte of LiPF₆-EC/PC/EMC (0.14/0.18/0.68). For LiFePO₄ electrode, 51.5% of its room temperature capacity is delivered at -30°C with the addition of 4% Li₂CO₃ in the electrolyte. As XPS measurement verified, the Li₂CO₃ precipitates on the electrode surface hinder electron transfer more efficiently and suppress electrolyte reaction further. Moreover, lithium ion migration within this phase is speeded up with the help of Li vacancies in Li₂CO₃.

Keywords: electrolyte modification, lithium carbonate, mass triangle model, lithium iron phosphate, low temperature

1. INTRODUCTION

The phospho-olivine LiFePO₄ material is currently under extensive studies due to its merits of long life, excellent thermal stability and high specific capacity of 170 mAh g⁻¹. Despite these features, the electrochemical performance of LiFePO₄ cathode is found to be less impressive at high charge/discharge rate and low temperature. The drawbacks are caused by the intrinsically poor ionic and electronic conductivities of LiFePO₄ with a unique olivine structure as Amin and Ouyang et al [1~3] pointed out. Therefore enhancing mass transport of Li⁺ is crucial to improve the capability of this material, especially at high rate and low temperature. The approaches to modify LiFePO₄ cathode performance are usually involved with two aspects, one is related to material modification, and the

other is electrolyte optimization. The most used methods for material modification are carbon coating [4,5], doping [6], nanocrystallization [7,8] and preferential growth of crystals [9]. Electrolyte optimization is concerned recently for its facile process and commercialization. It's reported that modifying solid electrolyte interphase (SEI) through electrolyte composition change is a way to improve the low temperature performance of LiFePO_4 electrode [10]. As temperature drops down, the migrations of lithium ions across the electrolyte and the interphase on active material are all increasingly hindered. Herein, the study on electrolyte conductivity and SEI film to ease the migration are of quite importance for LiFePO_4 performance improvement at low temperature.

Ethylene carbonate (EC)/ propylene carbonate (PC)/ ethyl methyl carbonate (EMC) were adopted as solvents according to the merits of each carbonate: high dielectric constant of EC (89.6), low melting point ($-48.8\text{ }^\circ\text{C}$) of PC and superior viscosity (0.65 mPa s^{-1}) of EMC. But there should be a compromise in the proportion of each solvent to obtain a high conductivity electrolyte. Mass triangle model was introduced to optimize the conductivity of lithium hexafluorophosphate (LiPF_6)-EC/PC/EMC (x/y/z, wt%) [11]. SEI film was modified with the addition of vinylene carbonate (VC) and Li_2CO_3 which are well known film forming additives for Li-ion battery [12,13]. Charge/discharge tests and cyclic voltammetry(CV) were conducted to examine the electrochemical performance of LiFePO_4 electrode in the electrolyte of EC/PC/EMC with VC or Li_2CO_3 additive . A big improvement is expected to fulfill on the LiFePO_4 electrode performance at low temperature so that its application could be extended to a wide temperature range.

2. EXPERIMENTAL

LiFePO_4 material was obtained from Reshine New Materials Co., Ltd., China and used without further modification. Its particle was in a size of 200-400 nm, having a carbon coating in a thickness around 5 nm. The electrode was prepared by spreading slurry of LiFePO_4 powder (80wt%), graphite (10wt%) and polyvinylidene fluoride (PVDF, 10wt%, dissolved in 1-methyl-2-pyrrolidinone) onto an aluminum foil. It was dried at $80\text{ }^\circ\text{C}$ for 20 h under vacuum prior to assembly. CR2025 coin cells were fabricated with lithium sheet as the counter electrode in an Ar-filled glove box. Ternary carbonate electrolytes with different EC/PC/EMC proportions were prepared in the glove box. The proportion of the solvent in each ternary electrolyte "No.1" to "No.10" was: (0.11, 0.59, 0.30), (0.12, 0.38, 0.50), (0.14, 0.18, 0.68), (0.25, 0.11, 0.64), (0.38, 0.12, 0.50), (0.39, 0.27, 0.34), (0.38, 0.39, 0.23), (0.24, 0.54, 0.22), (0.30, 0.30, 0.40), (0.25, 0.25, 0.50), respectively. The ratio values were determined according to the principle of conductivity forecast [14] by mass triangle modelling. 1wt% VC (Xianghe kunlun chemical products Co., LTD, China) or 4wt% Li_2CO_3 (99.9%, Aladdin Chemistry Co. Ltd, China) was used as electrolyte additive. Li_2CO_3 was hardly dissolved in the solvent, the modified electrolyte was used in the form of a homogeneous suspension.

Charge-discharge measurement was performed on CT2001A Land tester(Wuhan Jinnuo Electronics Co., Ltd.). After charged at 34 mA g^{-1} under room temperature, coin cells were preserved at desired temperatures for at least 2 h prior to discharging to 2.50 V at 17 mA g^{-1} . The electrolyte conductivity was measured using a conductivity meter (DDSJ-308A) through electrochemical

impedance spectroscopy (EIS) (100 Hz to 0.1 MHz, 5 mV perturbation) method. It's calculated by equation $\kappa=K/R$. Here, R represents the impedance value tested through EIS. K is the conductivity coefficient of the conductivity meter. κ is conductivity. Exchange current density was calculated from $j_0=10^{(-a/b)}$, a and b are the intercept and the slope of tafel curve, respectively. A polarization potential of 100 mV was applied on LiFePO₄ electrode which had been charged for 5 h under 17 mA g⁻¹ to ~3.425 V and left for 10 h to obtain a steady potential without any change in 100 s, i.e. 50% SOC(state of charge), to exert tafel plot test at 0.1 mV s⁻¹. CV, EIS and tafel plot test were performed using a CHI660c electrochemical station (Shanghai Chenhua Co. Ltd). A constant temperature chamber (Wuxi Suoyate Testing Equipment Co., Ltd., China) was used to maintain the desired temperature with an error of ± 0.5 °C.

After electrochemically cycled in various electrolytes for 10 times to delithiation state at room temperature, LiFePO₄ electrodes were disassembled from the coin cells and dried in vacuum before XPS or XRD tests. No solvent washing was adopted to keep the Li₂CO₃ precipitates on the electrode surface from washing away. XPS measurement was conducted on a PHI QUANTERA-II SXM system (Japan / Uivac-PHI, INC), using a monochromatised MgK α radiation source. The calibration of the peak position was made by recording XPS spectra of the graphite peak at 248.3 eV as the reference for the final adjustment of the energy scale. XRD test was carried out using X-ray diffractometer with a Cu K α radiation source at a scan rate of 8° min⁻¹, with 2θ from 10° to 80°. The wavelength of the Cu K α radiation used was 0.15406 nm. HOMO and LUMO energies of the matters on the surface were calculated with B3LYP density functional theory method in conjunction with the 6-31+G (d,p) basis set using Gaussian 09 package.

3. RESULTS AND DISCUSSION

The conductivities of electrolytes “No.1” to “No.10” were tested from 20 °C to -40 °C. The relationship between conductivity logarithm and temperature reciprocal is depicted in Fig.1. As shown in the curve, the conductivity of electrolyte “No.3” is the highest among the ten electrolytes, especially at -20 °C and -40 °C. But, the value is just limited in the ten samples. Mass triangle model was adopted to find out the highest conductivity through forecasting the conductivity of EC/PC/EMC system. The modelling was proceeded in a fixed area (shown in Fig.2) as the forecasting region because the electrolyte inside the region can guarantee the proper performance for electrode [14]. The changing tendency of conductivity as a function of solvent proportion at -40 °C is clearly seen in the forecasting region, which grows with EC decreasing and EMC increasing. The highest value reaches about 0.49 mS cm⁻¹ in the lower left part of the forecasting region where the composition of electrolyte “No.3” is coincidentally located. Therefore, No.3 (1 mol L⁻¹ LiPF₆-EC/PC/EMC = 0.14/0.18/0.68) is verified to own the highest conductivity in the applicable region in the EC/PC/EMC system, not only among the ten samples. So, it is used as the base electrolyte for further study.

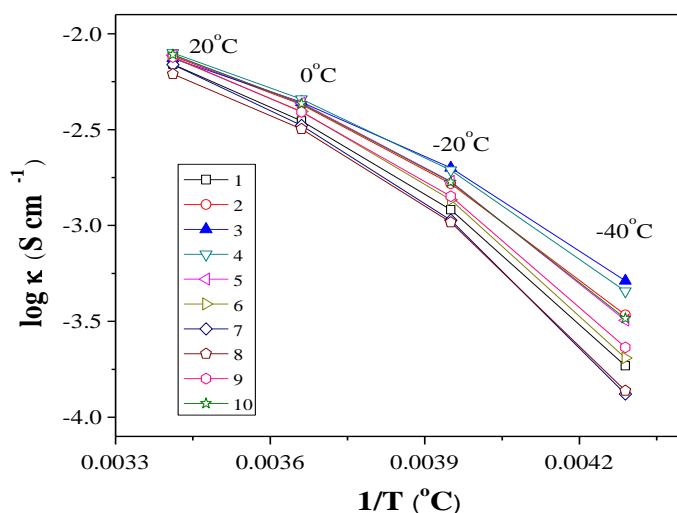


Figure 1. The relationships between conductivity logarithm and temperature reciprocal for electrolytes from “No.1” to “No.10”.

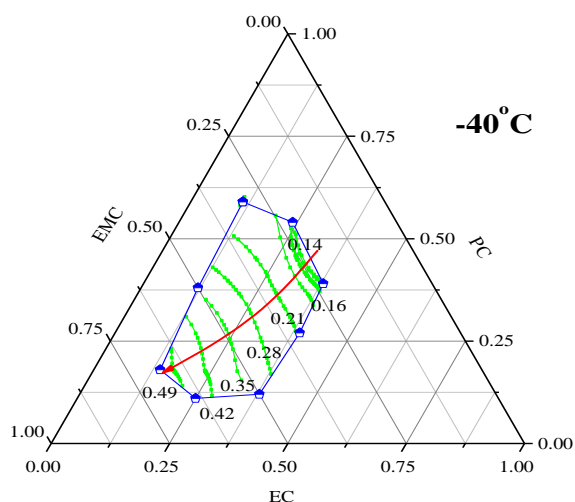


Figure 2. Calculated result at -40 °C according to mass triangle model (mS cm^{-1}). (the arrow indicates the increasing direction of conductivity).

Under room temperature, cyclic voltammograms of the LiFePO_4 electrodes in $1 \text{ mol L}^{-1} \text{ LiPF}_6\text{-EC/PC/EMC (0.14/0.18/0.68) (No.3)}$ without and with additive (VC or Li_2CO_3) are displayed in Fig.3. Compared with the additive free condition, the polarization of lithiation/delithiation is increased by the addition of VC in the electrolyte. The peak intensities become much lower, too. As a well known film-forming additive, VC doesn't behave well as reported upon some else cathodes [15, 16]. This result is consistent with the work of Ouatani [17] who also found VC did not make positive effect on LiFePO_4 electrode. In contrast to the VC-added case, Li_2CO_3 addition plays an active role according to the stronger peak intensities and weak polarization of delithiation (3.57 V) and lithiation (3.31 V) reactions.

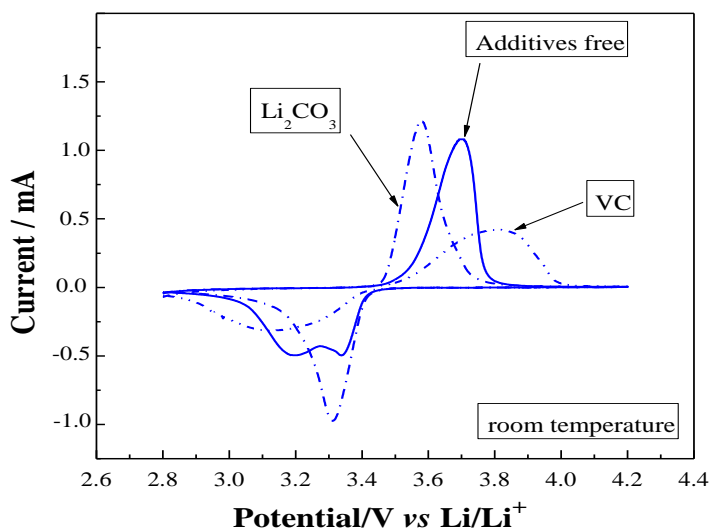


Figure 3. CV of LiFePO₄ electrode in 1 mol L⁻¹ LiPF₆/EC/PC/EMC (No.3) without and with additive (VC or Li₂CO₃) at a sweep rate of 0.1 mV s⁻¹ (the 2nd cycle, at room temperature)

Similarly, the weakened polarization phenomena also happen at low temperature, as shown in Fig.4. When Li₂CO₃ is added in the low temperature electrolyte, the reductive peak is shifted from 2.9 V to 3.0 V and the oxidative peak from 3.9 V to 3.8 V compared to the additive free condition. The potential difference of lithiation/delithiation is reduced by 200 mV in the presence of Li₂CO₃. Reversely, a negative effect appears with the addition of VC, as indicated in Fig.4. Much lower peak intensities and larger potential difference between delithiation (4.2 V) and lithiation (2.7 V) peaks are generated. Li₂CO₃ performs apparently superior to VC as electrolyte additive in this work. So, further efforts are done on the electrolyte modification with Li₂CO₃-additive to examine its contribution on the low temperature performance of LiFePO₄ electrode.

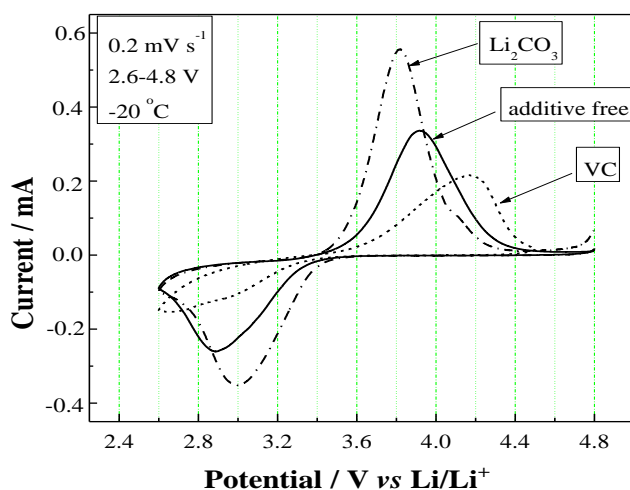


Figure 4. Cyclic voltammograms of LiFePO₄ electrode in 1 mol L⁻¹ LiPF₆/EC/PC/EMC (No.3) without and with different additives at a sweep rate of 0.2 mV s⁻¹ (-20 °C).

The discharge ability of the electrode in Li_2CO_3 added/free electrolytes was examined at low temperatures. The electrodes were first charged to 4.2 V at room temperature prior to the testing. Under $-20\text{ }^\circ\text{C}$, the capacity increase is observable in the presence of Li_2CO_3 , with a small increment (Fig.5(a)). At $-30\text{ }^\circ\text{C}$ in Fig.5(b), the discharge capacity of the electrode is only 47.2 mAh g^{-1} in the base electrolyte when the discharge potential falls down to 2.5 V. However, the specific capacity of the electrode rises by 63.6% to 77.2 mAh g^{-1} in the addition of Li_2CO_3 , i.e., 51.5% of its room temperature capacity (150 mAh g^{-1}) is delivered at $-30\text{ }^\circ\text{C}$. The potential difference between the two discharge curves is finally enlarged to 610 mV at the point showing in Fig5(b) (2.5 V and 3.11 V for the 0% and 4% Li_2CO_3 cases, respectively). It is indicated that the polarization of the electrode reaction is lowered with the addition of Li_2CO_3 . Clearly, the electrolyte additive of Li_2CO_3 can modify the electrochemical performance of LiFePO_4 electrode at low temperature.

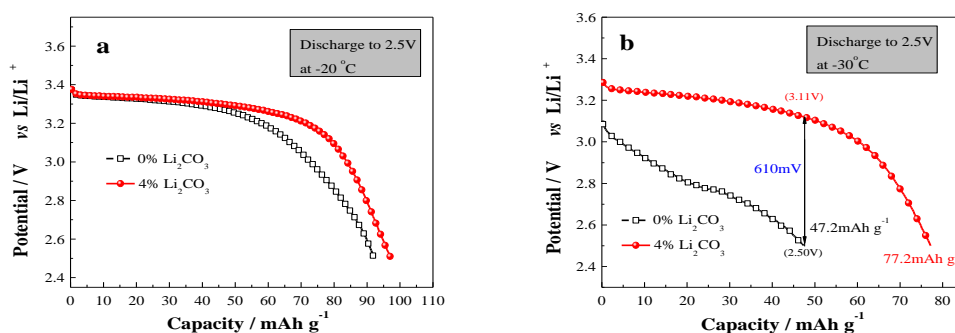


Figure 5. Discharge curves of LiFePO_4 in the electrolytes with 0% and 4% Li_2CO_3 at $-20\text{ }^\circ\text{C}$ (a) and $-30\text{ }^\circ\text{C}$ (b). (17 mA g^{-1} , cutoff potential: 2.5 V)

Charge transfer resistance (R_{ct}) is believed to be essential factor that associates with the low temperature performance of LIB. Small R_{ct} corresponds to big exchange current density (j_0) according to the equation $j_0 = RTF^{-1}R_{ct}^{-1}$. In this paper, the j_0 of LiFePO_4 electrode reaction was applied to judge the R_{ct} under the condition with Li_2CO_3 addition at various temperatures. As shown in Table 1, the exchange current densities are almost the same for the three electrolytes at room temperature, but the difference is enlarged as the temperature drops down. Especially at $-40\text{ }^\circ\text{C}$, the value in the presence of 4% Li_2CO_3 is 2.6 and 7.3 times as high as that of the additive free electrolyte and the conventional electrolyte ($\text{LiPF}_6\text{-EC/DMC}(1/1)$) (CE). The much lower value of j_0 for CE can be related to the electrolyte crystallization happened at $-40\text{ }^\circ\text{C}$. The crystallization severely hinders the mobility of Li^+ through the electrolyte, causing a dramatic drop of electrolyte conductivity, which also affects the charge transfer rate at the electrolyte/electrode interphase. The application of EC/PC/EMC (0.14/0.18/0.68) solvent system avoids the crystallization and obtains a high j_0 value of $3.69 \times 10^{-7}\text{ A cm}^{-2}$. Furthermore, the value is enhanced from $3.69 \times 10^{-7}\text{ A cm}^{-2}$ to $9.68 \times 10^{-7}\text{ A cm}^{-2}$ with the addition of Li_2CO_3 . So the impedance for the charge to transfer is decreased and the electrochemical reactivity of the electrode is increased in the presence of Li_2CO_3 at low temperature. Activation energy (E_a) for the charge transfer process as ca. 44.6 kJ mol^{-1} for the electrode in conventional electrolyte is derived

from the Arrhenius equation $\lg(j_0) = f(T^{-1})$ (Fig.6). However, for the electrolyte containing 4% Li_2CO_3 , the slope for the $\lg(j_0) = f(T^{-1})$ line gives the E_a of ca. 27.3 kJ mol^{-1} which is smaller than its Li_2CO_3 -free counterpart with the value of 34.0 kJ mol^{-1} . This result implies that the Li_2CO_3 additive can lower reaction barrier in the interphase between electrolyte and electrode. The improved performance of LiFePO_4 is ascribed to the weakened polarization and the small activation energy for the charge transfer process.

Table1. Exchange current densities of LiFePO_4 electrode in various electrolytes (A cm^{-2})

electrolytes	20 °C	-20 °C	-40 °C
$\text{LiPF}_6/\text{EC}/\text{PC}/\text{EMC}+0\% \text{ Li}_2\text{CO}_3$	1.42×10^{-5}	2.25×10^{-6}	3.69×10^{-7}
$\text{LiPF}_6/\text{EC}/\text{PC}/\text{EMC}+4\% \text{ Li}_2\text{CO}_3$	1.98×10^{-5}	7.47×10^{-6}	9.68×10^{-7}
Conventional ($\text{LiPF}_6/\text{EC}/\text{DMC}$)	1.76×10^{-5}	3.03×10^{-6}	1.32×10^{-7}

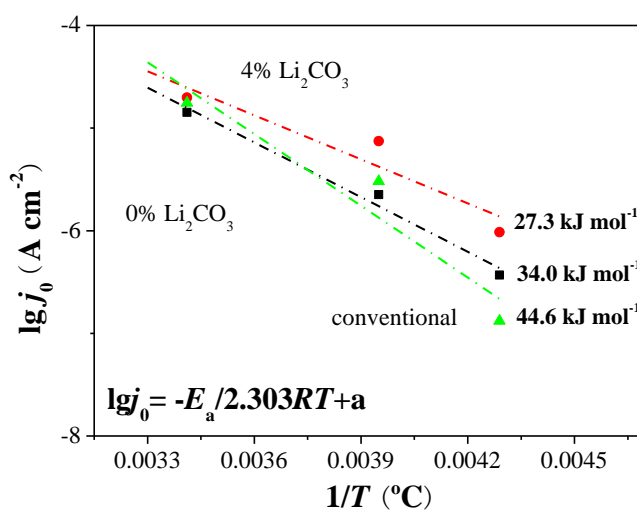


Figure 6. Arrhenius plots for exchange current density (j_0) obtained from measurement results in Table.1

Little morphology difference can be found in the scanning electron microscopy (SEM) images of the LiFePO_4 electrode cycled in the electrolyte with/without Li_2CO_3 . The component on LiFePO_4 electrode was investigated by XPS further. Fig.7 reveals various species on the cathode surface in both 0% and 4% Li_2CO_3 addition cases. Intensities of C-O bond (286.4 eV) and C=O bond (289.8 eV) decrease with the addition of Li_2CO_3 , as C1s spectra implied. The result is also consistent with the C-O and C=O peaks at 533.5 eV and 531.5 eV in O1s spectra. Additionally, O1s spectra show a strong peak of CO_2^- at 532.4 eV. The major peaks in F1s spectra represent LiF (685.0 eV) and PVDF (687.6 eV) for the Li_2CO_3 -free case. However, C-F₂ peak at 688.2 eV dominates the spectra in the Li_2CO_3 -added case, the content of LiF in the interphase is largely lessened. LiF is verified to be highly resistive by many researchers [18-21], and the decrease of its amount is beneficial for the migration of lithium ion. The

P2p spectra contains the peaks of $\text{Li}_x\text{PO}_y\text{F}_z$ (134.2 eV), OPF_3 (135.6 eV), Li_xPF_y (137 eV). The peak intensity of OPF_3 is higher in the 4% Li_2CO_3 case. Tasaki et al [22] also detected the existence of OPF_3 through ^{19}F -NMR method. OPF_3 may come from the decomposition of LiPF_6 and the product of reactions among Li_2CO_3 , RCO_2Li and PF_5 according to equations (1) to (4).

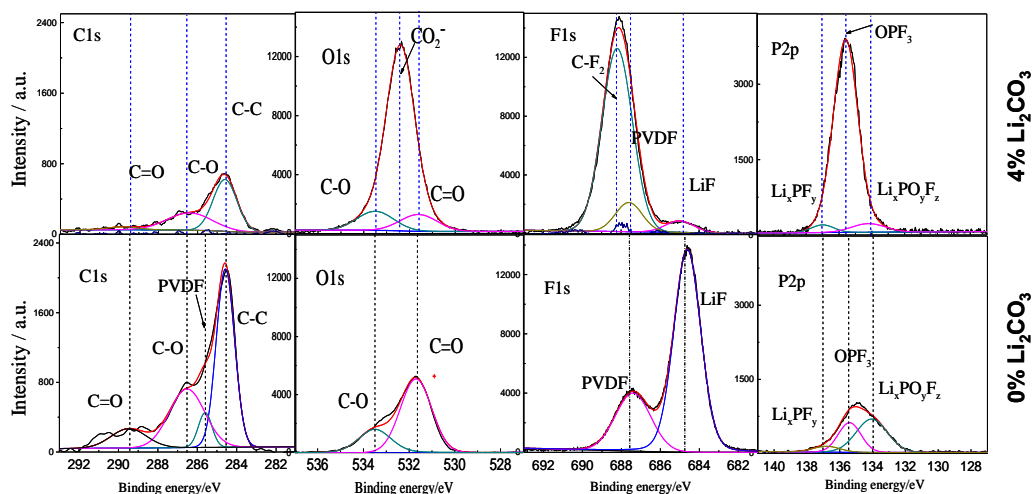


Figure 7. XPS spectra for delithiated LiFePO_4 electrode after cycled in the electrolyte containing 4% (top) and 0% (bottom) Li_2CO_3 .

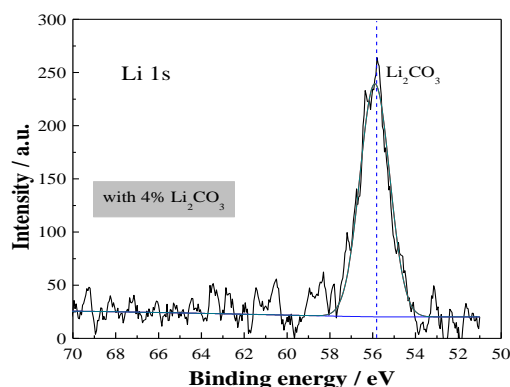
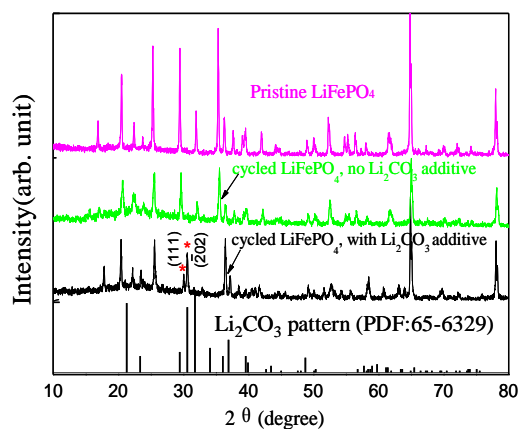
The species containing C-O and C=O bonds are ascribed to the decomposition product of alkyl carbonate solvents during the insertion/extraction of lithium ion. However, the contents of these matters decrease upon adding 4% Li_2CO_3 based on their low intensities in the XPS spectra, which confirm that decomposition of the alkyl carbonate solvents is suppressed. Li_2CO_3 was reported to be less conductive for electrons because of its wide forbidden band gap [23]. Reasonably, it is supposed that the low intensity of C-O and C=O may be caused by the formation of Li_2CO_3 -contained interphase which is of better prohibitive to electronic conduction on the LiFePO_4 surface to suppress solvents decomposition.

As a Lewis acid, PF_5 displays a strong acidity as indicated by a very low LUMO energy level in Table 2. In the presence of Li_2CO_3 , PF_5 is more likely to react with Li_2CO_3 rather than RCO_2Li since the HOMO energy of Li_2CO_3 (-0.24051 Hartree) is closer to the LUMO energy of PF_5 (-0.04904 Hartree). Thereby, RCO_2Li is less consumed and remains much in the case of Li_2CO_3 addition. The existence of RCO_2Li can also be verified by the high intensity of the peak CO_2^- at 532.4 eV in O1s spectra.

Table 2. HOMO and LUMO energies of the species on the electrode surface

chemicals	HOMO(Ha)	LUMO(Ha)
PF ₅	-0.43941	-0.04904
Li ₂ CO ₃	-0.24051	-0.03660
RCO ₂ Li	-0.26120	-0.03762
CH ₃ CO ₂ Li	-0.26122	-0.03743
CH ₃ CH ₂ CO ₂ Li	-0.26122	-0.03743

XPS Li1s spectra in Fig.8 indicate that Li₂CO₃ is detectable on the surface of LiFePO₄ electrode cycled in the electrolyte with Li₂CO₃ additive. XRD test was also conducted on the LiFePO₄ electrode which had the same charge/discharge history with the one in XPS analysis. Li₂CO₃ is found according to the peaks of (111) and ($\bar{2}$ 02) at 30.0° and 30.5° in the Li₂CO₃-added case, as seen in Fig.9.

**Figure 8.** Li1s XPS spectra of LiFePO₄ electrode cycled in the electrolyte with 4% Li₂CO₃.**Figure 9.** The XRD pattern of pristine LiFePO₄ and the electrode (delithiated state) cycled in the electrolyte with/without Li₂CO₃.

Actually, some white precipitates were clearly visible on the cathode surface as well when the coin cell was disassembled in the experiment. The energy barrier for single lithium ion diffusion in Li_2CO_3 is close to (or even somewhat lower than) that of its diffusion in bulk graphite according to DFT calculation [23]. Li_2CO_3 is thought a superior medium for Li^+ migration since the diffusion is very fast in Li_2CO_3 with the help of Li vacancies. So, lithium ion migration through the interphase is facilitated generating a decreased electrode polarization at low temperature as tested above (Fig.5).

The modified SEI film hinders electron transport and facilitates lithium ion migration, leading to less electrolyte decomposition and faster lithiation/delithiation reactivity. As a result, the low temperature performance of LiFePO_4 electrode is improved with the SEI film modification together with the electrolyte conductivity enhancement. Li_2CO_3 is hence a potential electrolyte additive for LiFePO_4 battery to widen its application.

4. CONCLUSIONS

An optimized solvent proportion of EC/PC/EMC (0.14, 0.18, 0.68) is obtained for a low temperature electrolyte ($1 \text{ mol L}^{-1} \text{ LiPF}_6$) with high conductivity by mass triangle modelling. The discharge capacity of 77.2 mAh g^{-1} for LiFePO_4 electrode is achieved at $-30 \text{ }^\circ\text{C}$ with 4% Li_2CO_3 additive in the electrolyte of LiPF_6 -EC/PC/EMC (0.14, 0.18, 0.68). Li_2CO_3 -contained interphase is formed on the LiFePO_4 electrode cycled in the electrolyte with Li_2CO_3 . The modified SEI film effectively hinders the electron transport due to the wide forbidden band gap of Li_2CO_3 , and facilitates lithium ion migration with the help of Li vacancies in Li_2CO_3 . Electrolyte decomposition reaction is also suppressed by the Li_2CO_3 -contained interphase. Consequently, the electrochemical performance of LiFePO_4 electrode is improved with the weak polarization and the low activation energy for the charge transfer process in the presence of Li_2CO_3 which is considered a most positive component in the SEI film and a potential electrolyte additive.

ACKNOWLEDGEMENTS

This project was financially supported by the National 973 Program (Grant No. 2009CB220100) and the National 863 Program (2013AA050903) of China, the National Natural Science Foundation of China (3100021501101) and Ministry of Science and Technology (MOST) of China, US-China Collaboration on cutting-edge technology development of electric vehicle (2010DFA72760).

References

1. R. Amin, P. Balaya and J. Maier, *Electrochem. Solid-State Lett.* 10 (2007) A13.
2. C.Y. Ouyang, S.Q. Shi, Z.X. Wang, X.J. Huang and L.Q. Chen, *Phys. Rev. B*, 69 (2004) 1.
3. C.Y. Ouyang, S.Q. Shi, Z.X. Wang, H. Li, X.J. Huang and L.Q. Chen, *J. Phys. Condens. Matter.*, 16 (2004) 2265.
4. A. Yamada, S.C. Chung and K. Hinokuma, *J. Electrochem. Soc.*, 148 (2001) A224.
5. H.C. Shin, W.I. Cho and H. Jang, *Electrochim. Acta*, 52 (2006) 1472.
6. S.Y. Chung, J.T. Bloking and Y.M. Chiang, *Nat. Mater.*, 1 (2002) 123.

7. A.S. Aricò, P. Bruce, B. Scrosati, J.M. Tarascon and W.V. Schalkwijk, *Nat. Mater.*, 4 (2005) 366.
8. S. Ferrari, R.L. Lavall, D. Capsoni, E. Quartarone, A. Magistris, P. Mustarelli and P. Canton, *J. Phys. Chem. C*, 114 (2010) 12598.
9. M.S. Islam, D.J. Driscoll, C.A.J. Fisher and P.R. Slater, *Chem. Mater.*, 17 (2005) 5085.
10. D.P. Abraham, J.R. Heaton, S.H. Kang, D.W. Dees and A.N.J. Jansen, *J. Electrochem. Soc.*, 155 (2008) A41.
11. J.Y. Huang, B.T. Yu, F.S. Li and W.H. Qiu, *Int. J. Miner. Metall. Mater.*, 16 (2009) 463.
12. Y.X. Wang and P.B. Balbuena, *J. Phys. Chem. B*, 106 (2002) 4486.
13. D. Aurbach, Y. Ein-Eli, B. Markovsky, A. Zaban, S. Luski, Y. Carmeli and H. Yamin, *J. Electrochem. Soc.*, 142 (1995) 2873.
14. Y.H. Ren, B.R. Wu, D.B. Mu, C.W. Yang, C.Z. Zhang and F. Wu, *Chem. Res. Chin. Univ.*, 29 (2013) 116.
15. K. Sato, L.W. Zhao, S. Okada and J. Yamaki, *J. Power Sources*, 196 (2011) 5617.
16. X.R. Zhang, R. Kosteci, T.J. Richardson, J.K. Pugh and P.N. Ross, *J. Electrochem. Soc.*, 148 (2001) A1341.
17. L.El Ouatani, R. Dedryvère, C. Siret, P. Biensan and D. Gonbeau, *J. Electrochem. Soc.*, 156 (2009) A468.
18. A.J. Gmitter, I. Plitz and G.G. Amatucci, *J. Electrochem. Soc.*, 159 (2012) A370.
19. K. Xu, *Chem. Rev.*, 104 (2004) 4303.
20. Y.K. Sun, J.M. Han, S.T. Myung, S.W. Lee and K. Amine, *Electrochem. Commun.*, 8 (2006) 821.
21. D. Aurbach, B. Markovsky, A. Rodkin, E. Levi, Y.S. Cohen, H.J. Kim and M. Schmidt, *Electrochim. Acta*, 47 (2002) 4291.
22. K. Tasaki, K. Kanda, S. Nakamura and M. Ue, *J. Electrochem. Soc.*, 150 (2003) A1628.
23. Y.C. Chen, C.Y. Ouyang, L.J. Song and Z. L. Sun, *J. Phys. Chem. C*, 115 (2011) 7044.